Modulating Carrier Dynamics through Perovskite Film Engineering

Lim, Swee Sien; Chong, Wee Kiang; Solanki, Ankur; Dewi, Herlina Arianita; Mhaisalkar, Subodh Gautam; Mathews, Nripan; Sum, Tze Chien

2016

Lim, S. S., Chong, W. K., Solanki, A., Dewi, H. A., Mhaisalkar, S. G., Mathews, N., et al. (2016). Physical Chemistry Chemical Physics, in press.

https://hdl.handle.net/10356/81493

https://doi.org/10.1039/C6CP02640K

Journal Name

ARTICLE

Modulating Carrier Dynamics through Perovskite Film Engineering

Swee Sien Lim[a,b], *Wee Kiang Chong*[a,b], *Ankur Solanki*[b], *Herlina Arianita Dewi*[c], *Subodh Mhaisalkar*[c,d], *Nripan Mathews*[c,d]†, *and Tze Chien Sum*[b]†

Received 00th January 20xx,
Accepted 00th January 20xx

DOI: 10.1039/x0xx00000x

www.rsc.org/

Precise morphological control in perovskite films is key to high performance photovoltaic and light emitting devices. However, a clear understanding of the interplay of morphological effects from substrate/perovskite antisolvent treatments on the charge dynamics is still severely lacking. Through detailed ultrafast optical spectroscopy, we correlate the morphology-kinetics relationship in a combination of substrate/film treated samples (*i.e.*, plasma-cleaned vs piranha-etched substrates and solvent (toluene)-engineered (or toluene anti-solvent treated) perovskite films). Our findings reveal that toluene-dripped treatment has a more pronounced influence on the morphology of perovskite films prepared on plasma-cleaned substrates over those on piranha-etched substrates. Surprisingly, the highly effective toluene-dripping/washing approach reported in the literature increases the surface trap densities of perovskite films. Despite the marked improvements in the surface morphology of the toluene-dripped films, there is only a slight improvement in the carrier relaxation lifetimes – likely due to the competition between the morphology improvements and the increased surface traps densities. In addition, the injection of photoexcited holes to spiro-OMeTAD from toluene-dripped films on piranha-etched substrates is inhibited, possibly due to a realignment of the energy bands. Nonetheless, piranha-etching of the substrates could possibly offer an approach to improve the balance between the electron and hole diffusion lengths in the perovskite film. Importantly, our findings would help unravel the complex relationship of substrate/film treatments on the morphology and charge kinetics in perovskite thin films.

Introduction

Organic-inorganic hybrid perovskites have attracted immense attention primarily due to its outstanding photovoltaic and light emission properties. Specifically, certified power conversion efficiencies exceeding 20% have been demonstrated in perovskite solar cells – attributed to their large absorption coefficients and long, balanced, ambipolar diffusion lengths[1, 2] and large grains[3]. Recently, $CH_3NH_3PbI_3$ phototransistors that works in both accumulation and depletion modes were demonstrated, highlighting the importance of ambipolar transport[4]. Furthermore, $CH_3NH_3PbBr_3$ light-emitting diodes with >8% external quantum efficiencies were also reported – attributed to the suppression of metallic lead atoms and the spatial confinement of excitons in small, uniform nanograins[5]. The ubiquity, ease of use, and low cost solution-proccesability of these perovskite devices are their key attractiveness. However, one major issue of solution processing is the careful morphological control needed to form dense, uniform films essential for high performance photovoltaic and light emitting devices (LEDs). Poor film coverage would result in decreased light absorption and increased shunting pathways in photovoltaics[6]; while resulting in current leakage and poor exciton confinement in LEDs[5] that leads to adverse device performance. A myriad of factors can affect perovskite film morphology ranging from: the deposition method (single[7, 8] vs two-step deposition[9]), substrate wettability[6], and subsequent film modifications[10, 11]. Substrate treatment is necessary since the perovskite solution does not readily wet the substrate's surface. Typical semiconductor processing approaches to improve surface hydrophilicity include plasma-cleaning and piranha-etching of substrates; where the former is commonly used in perovskite devices, and the latter in the silicon industry. Despite both photovoltaic and LED applications require dense, uniform films[12], there are in fact contrasting morphological criteria (*i.e.*, large crystals in the former but small nanograins in the latter). Detailed insights into the intricate relationship between substrate and film treatments on morphology and the ensuing charge kinetics are still severely lacking.

Here, we performed a comprehensive ultrafast optical spectroscopy study of various substrate/film-treated perovskite thin films (*i.e.*, plasma-cleaned vs piranha-etched

[a] *Energy Research Institute @NTU (ERI@N), Interdisciplinary Graduate School Nanyang Technological University, Singapore Address here.*
[b] *School of Physical and Mathematical Sciences, Nanyang Technological University, 21 Nanyang Link, 637371, Singapore*
[c] *Energy Research Institute @NTU (ERI@N), Research Techno Plaza, X-Frontier Block, Level 5, 50 Nanyang Drive, Singapore 637553*
[d] *School of Materials Science and Engineering Nanyang Technological University Nanyang Avenue, 639798, Singapore*
† Corresponding authors. Email: Tzechien@ntu.edu.sg (T.C.S), Nripan@ntu.edu.sg (N.M.)
Electronic Supplementary Information (ESI) available: Experimental methods and materials synthesis. XRD and TA spectra of the various perovskite films, TRPL and steady-state PL of perovskite films with quenching layers. See DOI: 10.1039/x0xx00000x

quartz substrates and with toluene drip) in a bid to investigate the structure-functional relationship by correlating the effects of morphology with the carrier dynamics. Insulating quartz substrates were used in this study for a non-injecting interface to avoid influence on the charge kinetics. Surprisingly, our findings reveal that solvent engineering of perovskites, which is key to improving film morphologies and subsequent solar cell efficiencies, had resulted in increased trap densities. We attribute this anomalous behavior to an interplay of factors where the improved film morphology (after solvent engineering of the perovskites on the plasma-cleaned substrates) had also resulted in the lengthening of the carrier recombination lifetimes.

Results

In an attempt to discern the influence of the substrate treatment and solvent engineering (henceforth termed film treatment) on the morphology, two different types of substrate treatments were used prior to single-step perovskite solution spincoating; namely, air plasma-cleaning, and piranha-etching, denoted with prefixes *Plas* and *Pir*, respectively. Standard samples, *i.e.*, without toluene drip, are denoted with suffix *S*. Another pair of quartz substrates with the same treatments had toluene dripped 5 seconds into the perovskite spincoating process, denoted with suffix *T*. Dripping with toluene was previously shown to be an effective film engineering approach that would markedly increase the surface coverage of the film[10, 11]. Figure 1 depicts SEM and AFM images (AFM images processed using WSxM[13] to estimate Root-Mean-Squared roughness, Rq) of the different samples with varying fabrication conditions on both substrate and film. In our study, thin 10 wt. % films, having an optical density (OD) ~0.2, are used to fulfil the thin sample approximation for pump-probe spectroscopy. X-ray diffraction patterns show that these treatments do not affect the crystallinity of the annealed $CH_3NH_3PbI_3$ films (Figure S1 in supporting information), but all treatments other than Plas-S resulted in a decrease in crystallite size (Table S1).

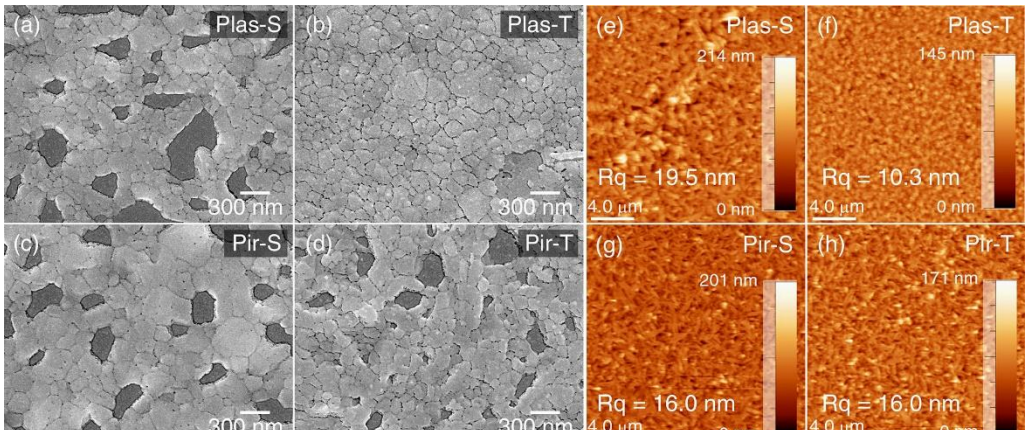

Figure 1. SEM (a,b,c,d) and AFM (e,f,g,h) images of neat $CH_3NH_3PbI_3$ perovskite films on quartz with various substrate and film treatment: (a, e) Plas-S, (b, f) Plas-T, (c, g) Pir-S, and (d, h) Pir-T. Prefixes Plas denotes plasma-cleaned quartz, and Pir denotes piranha-etched quartz. Suffixes S denotes standard samples (i.e., without toluene drip), and T denotes samples with toluene drip, dripped 5 seconds from the start of the spincoating. The size of the AFM images is 20 by 20 μm^2.

The perovskite spuncoated on plasma-cleaned quartz (Plas-S, Figure 1a, e, Rq = 19.5 nm) is used as the reference for comparison. The addition of toluene during the spincoating process evidently decreases surface roughness (Plas-T, Figure 1b, f, Rq = 10.3 nm) of the perovskite film. As expected, the perovskite film covers the surface of the substrate very well. Spincoating the perovskite on piranha-etched films (Pir-S, Figure 1c, g, Rq = 16.0 nm) reduced surface roughness slightly, with no obvious improvement in coverage. Perovskite films spuncoated on piranha-etched quartz with toluene drip (Pir-T, Figure 1d, h, Rq = 16.0 nm) did not seem to reduce surface roughness (under similar experimental conditions) and had no observable improvements to the surface morphology. This is in stark contrast to the perovskite film morphology grown on plasma-cleaned sample (top row of Figure 1). Next, we examine charge dynamics of the samples using femtosecond transient absorption spectroscopy (fs-TAS).

The TA spectra at different time delays for Plas-S are shown in Figure 2a (see Figure S2 for TA spectra of other samples). Three distinct spectral features typical of photoexcited $CH_3NH_3PbI_3$ perovskite films are evident where the strongest positive ΔT signal (a positive differential transmission denotes photobleaching, whereas a negative differential transmission denotes photoinduced absorption) at ~770 nm (PB2) is attributed to bandedge photobleaching and stimulated emission. Currently, it is still an open debate over the origins of the weaker photobleaching band at ~480 nm (PB1), with interpretations of the origins from the dual valence band/dual conduction bands[1, 14] (see Figure 2b inset and Figure S2) and/or overlapping contributions from PbI_2[15]. A recent work attributed the broad photoinduced absorption between PB1 and PB2 to originate from photoinduced refractive index changes[16]. To assess the carrier recombination as a result of substrate/film modification, bandedge (PB2) TA kinetics of the photoexcited samples as a function of pump and probe delay is

extracted and shown in Figure 2b. A pump wavelength of 600 nm at a relatively low fluence (5 μJ cm^{-2}) was used to excite the carriers across the bandgap and avoid multi-particle interactions, while still maintaining good signal-to-noise ratio. The TA signal was fitted with a multi-exponential function (with the system response deconvolved) to account for both the rise, and the mono-exponential decay for the carrier relaxation. Such mono-exponential decay obtained at low pump excitation is typical of a trap-dominated recombination. The rise in the ΔT signal is attributed to the hot-carrier cooling[14] and state-filling of the bandedge states. A comparison of the TA signals from the four samples would allow us to gain insights into the time evolution of the population of the photoexcited states within the perovskites films that have undergone different film and substrate treatments.

The marked improvement of morphology in Plas-T when compared to Plas-S accounts for the lifetime lengthening evident in Figure 2b, where $\tau_{Plas\text{-}T}$ = 9.9 ± 0.2 ns vs $\tau_{Plas\text{-}S}$ = 8.6 ± 0.1 ns. As the measurement window of our delay stage is limited to ~5ns, these fitted values should not be taken with absolute certainty. Nonetheless, one can still qualitatively compare the influence of the substrate/film treatments on the trend of the recombination lifetimes. Such lifetime lengthening is in agreement with past reports that films with better morphology exhibits longer lifetimes[17]. Comparatively, the films with piranha-etched substrates yielded a faster recombination over those with plasma treatment. Despite the slight improvement in morphology that Pir-S has over Plas-S, the former's lifetime is still considerably quenched. Surprisingly, the recombination lifetimes in toluene-washed films on piranha-etched substrates are severely quenched (Figure 2b, Pir-S: 7.0 ± 0.1 ns vs. Pir-T: 4.1 ± 0.1 ns); in contrast to films on plasma-treated substrates.

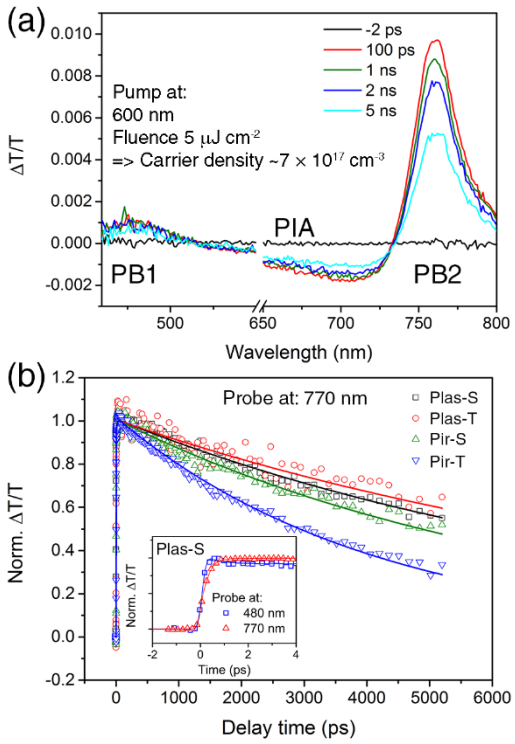

Figure 2. (a) TA spectra at various time delays of Plas-S $CH_3NH_3PbI_3$ perovskite sample pumped at 600 nm with a fluence of 5 μJ cm^{-2}. This is the typical spectra of all $CH_3NH_3PbI_3$ perovskite thin films. (b) Normalized TA kinetics of the $CH_3NH_3PbI_3$ samples: Plas-S (black square), Plas-T (red circle), Pir-S (green triangle), and Pir-T (blue inverted triangle). Solid lines are the fit results obtained from deconvolution fitting. Inset: Early-time dynamics of Plas-S, showing the simultaneous rise of the 770 nm trace and the fall of the 480 nm trace – evidence of hot-carrier cooling. The various substrate/film treatments has not affected these early time dynamics – see Figure S2 for details.

Given that the piranha-etched samples (i.e. Pir-S and Pir-T) are largely similar in surface morphology, evident from both AFM and SEM images (bottom row of Figure 1), we posit that the lifetime quenching is not solely a consequence of the induced morphological changes, but could possibly arise from the introduction of additional non-radiative recombination channels following the addition of toluene during the spin-coating process.

To ascertain the cause for the quenching, we performed power dependent steady-state photoluminescence in the low fluence regime (where there is negligible Auger recombination) to estimate the trap densities.

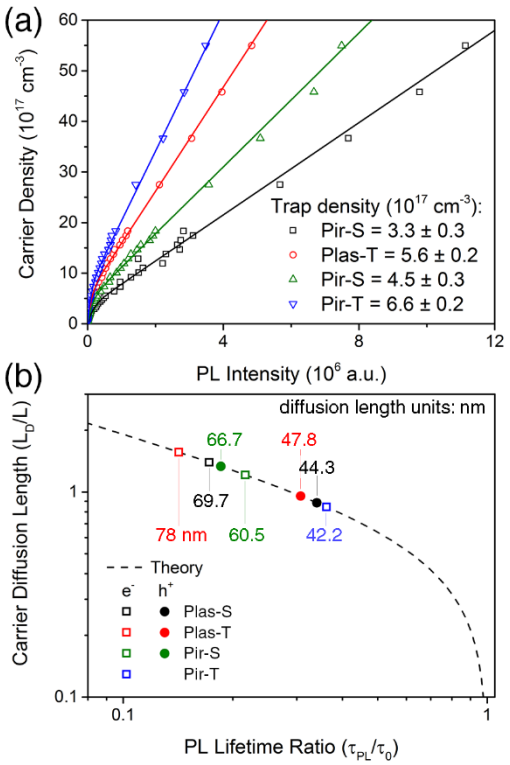

Figure 3. (a) Photoexcited carrier density as a function of PL intensity for the various $CH_3NH_3PbI_3$ samples: PLAS-S (black square), Plas-T (red circle), Pir-S (green triangle), and Pir-T (blue inverted triangle). The experimental data is fitted with our trap density model and are assigned to surface traps. (b) Normalized carrier diffusion lengths as a function of the PL quenching ratios for the various $CH_3NH_3PbI_3$ samples with electron quencher (open square), or hole quencher (closed circle) calculated from Equation 1 (dashed line). The diffusion lengths are normalized to the thickness of the perovskite films.

The trap densities of the samples are estimated using a model developed in an earlier work[18], and the results are summarized in Figure 3. Briefly, the model assumes an infinite number of trapping pathways, each with their distinct trapping rates and trap densities. From Figure 3a, we observe the trap densities (N_t): Plas-S has the lowest trap density $N_{t,Plas\text{-}S}$ = (3.3 ± 0.3) × 10^{17} cm^{-3}; followed by Pir-S, $N_{t,Pir\text{-}S}$ = (5.6 ± 0.2) × 10^{17} cm^{-3}; Plas-T, $N_{t,Plas\text{-}T}$ = (4.5 ± 0.3) × 10^{17} cm^{-3} and; Pir-T, $N_{t,Pir\text{-}T}$ = (6.6 ± 0.2) × 10^{17} cm^{-3}. Although our model can discern between bulk and surface traps, the data could be well-fitted by just considering only one type of trap. The traps are primarily surface-related, possibly MA vacancies[19], since the dripping of toluene is expected to have a larger impact on the surface of the perovskite[20]. This does not imply that bulk traps do not exist, but the density may be much smaller than that of surface traps. Based on the work by Jeon *et al.*[10] and Xiao *et al.*[11], it has been generally accepted that solvent engineering (i.e. toluene-drip) results in better film morphology. Surprisingly, our findings reveal that toluene dripping actually increases the trap densities (that quenches the carrier relaxation) in the perovskite films regardless of substrate treatments. For piranha-etched substrates, although the perovskite film morphology remains unaltered with toluene dripping, the carrier dynamics become significantly quenched. For plasma-cleaned substrates, the perovskite film morphology is significantly improved with toluene dripping and the carrier dynamics were improved in stark contrast to piranha-etched substrates. Although the addition of toluene during the spincoating process introduces traps into the perovskite film, this is counteracted by the large improvement in film morphology. This explains why there is only a small improvement in the carrier lifetime, as the effects of film morphology and trap density are competing with each other and the interplay of these two factors heavily influence carrier relaxation mechanisms within films.

Another important parameter for assessing the impact of the substrate/film treatments would be the diffusion length of charge carriers in the presence of electron and hole quenching layers, PCBM and spiro-OMeTAD respectively. A summary of the results is shown in Figure 3b. The electron and hole diffusion lengths were estimated by extracting the time-resolved photoluminescence lifetimes (Figure S3) using a 1D diffusion length model[1] (see SI for derivation):

$$\frac{L_D}{L} = \frac{2}{\pi}\sqrt{\frac{1}{\frac{\tau_D}{\tau_0}} - 1} \qquad \text{- Equation 1}$$

where L_D is the diffusion length, L is the sample thickness, τ_D and τ_0 are the fitted monoexponential lifetimes with and without quencher layer respectively. From Equation 1, it is important to note that the estimated diffusion lengths are strongly influenced by the actual thickness of the sample. The estimated diffusion lengths are reasonable since our samples are roughly ~50 nm thick. One should not expect micron diffusion lengths like in large mm sized perovskite single crystals[21, 22] and it would be highly unreliable to extrapolate our results.

Figure 3 illustrates the normalized diffusion lengths of the perovskite samples – normalized to the thickness of the samples for comparison. In the case of Plas-S and Plas-T, the electron and hole diffusion lengths remain relatively invariant after toluene dripping. Comparing the Plas-S and Pir-S samples, the electron and hole diffusion lengths in the piranha-etched substrates are more balanced. As in the case for Pir-S and Pir-T, the combination of substrate and film treatments strongly influences charge dynamics and the diffusion lengths. The electron diffusion length is considerably shortened by 1/3 with toluene drip in Pir-T over Pir-S. However, the hole diffusion length cannot be estimated because of the absence of any lifetime quenching from the Pir-T sample. Due to the non-conductive nature of the quartz substrate, we were unable to measure the energy band alignments using XPS. As mentioned earlier, quartz substrates were used here in this study as a non-injecting interface. The piranha-etching, together with toluene-drip may have modified the substrate/film interface and formed an interfacial barrier[23] between the perovskite film and the spiro-OMeTAD hole quencher which prevents extraction of the holes. This is evident when we consider the lengthening of PL lifetime and enhancement of PL in Pir-T spiro-OMeTAD samples.

A recent work by Cohen *et al.* found that toluene-treated perovskite films were slightly more intrinsic (*i.e.*, more p-type with the Fermi level less negative by 0.1 eV) than non-treated films based on surface photovoltage measurements[19]. The n-

type perovskite film allows extraction of holes under normal circumstances, but as piranha-etching and toluene dripping of the films likely induce p-type behavior, the Fermi level is then shifted to be equal or below that of the spiro-OMeTAD, leading to poor/non-injecting scenarios – see Figure S5 for details. This shift in the Fermi level can be a result of MA (methylammonium, or CH_3NH_3 organic cation) defects (vacancies, interstitials and substitutions) that was previously shown with density functional theory calculations by Yin *et al*[24]. A lower defect formation energy indicates a higher probability of the defect existing and dripping with toluene increased the density of MA vacancies[19] which are acceptors in nature[24]. While we are not able to identify the specific type of defects introduced in our samples, the observed increase in trap density in toluene-dripped films and the poor/non-injecting behavior of Pir-T suggests that MA vacancies may be responsible, and agrees well with literature. The non-injecting behavior makes the combination of piranha-etching and toluene dripping unfavorable for both PV and LED applications. On the other hand, the electron and hole diffusion lengths are more balanced on piranha-etched substrates, which is also beneficial in other optoelectronic applications like phototransistors[4].

Conclusions

In summary, our findings reveal new insights into the convoluted relationship over the substrate/film treatments on the film morphology and the ensuing carrier recombination dynamics, defect densities and carrier diffusion lengths. The addition of toluene during the spincoating process was shown to improve film uniformity. Our results clearly demonstrate that not all treatments are suitable: *e.g.*, the surface trap densities in toluene-dripped samples are much higher than standard samples; and for films fabricated on piranha-etched substrates, which leads to poor hole extraction. Nonetheless, piranha-etching of the substrates could possibly offer an approach to improve the balance between the electron and hole diffusion lengths in the perovskite film. One must therefore exercise prudence in choosing appropriate treatments during sample fabrication. Although new insights could be gained by studying the charge dynamics, it is important to note that a device with different charge transporting layers and interfaces are significantly more complex than the bare films studied here. While it would be myopic to draw strict conclusions from the findings in thin films and extend them to real devices, we anticipate that with improvements in growth techniques, together with sedulous modulation of the perovskite morphology through a judicious choice in substrate/film treatments is key to the scaling-up of high efficiency perovskite devices.

Acknowledgements

Financial support from Nanyang Technological University start-up grants M4080514 and M4081293; the Singapore Ministry of Education Ministry of Education Academic Research Fund Tier 1 grants RG184/14 and RG101/15 and Tier 2 grants MOE2013-T2-1-081 and MOE2014-T2-1-044; the NTU-A*STAR Silicon Technologies Center of Excellence Program Grant 11235100003 and from the Singapore National Research Foundation through the Singapore–Berkeley Research Initiative for Sustainable Energy (SinBeRISE) CREATE Program and the Competitive Research Program NRF-CRP14-2014-03 is gratefully acknowledged. The authors would like to acknowledge Dr Xu Qiang for the insightful discussions on the density functional theory calculations.

Notes and references

1. G. Xing, N. Mathews, S. Sun, S. S. Lim, Y. M. Lam, M. Grätzel, S. Mhaisalkar and T. C. Sum, *Science*, 2013, **342**, 344-347.
2. S. D. Stranks, G. E. Eperon, G. Grancini, C. Menelaou, M. J. P. Alcocer, T. Leijtens, L. M. Herz, A. Petrozza and H. J. Snaith, *Science*, 2013, **342**, 341-344.
3. W. Nie, H. Tsai, R. Asadpour, J.-C. Blancon, A. J. Neukirch, G. Gupta, J. J. Crochet, M. Chhowalla, S. Tretiak, M. A. Alam, H.-L. Wang and A. D. Mohite, *Science*, 2015, **347**, 522-525.
4. F. Li, C. Ma, H. Wang, W. Hu, W. Yu, A. D. Sheikh and T. Wu, *Nature communications*, 2015, **6**, 8238-8238.
5. H. Cho, S.-H. Jeong, M.-H. Park, Y.-H. Kim, C. Wolf, C.-L. Lee, J. H. Heo, A. Sadhanala, N. Myoung, S. Yoo, S. H. Im, R. H. Friend and T.-W. Lee, *Science*, 2015, **350**, 1222-1225.
6. G. E. Eperon, V. M. Burlakov, P. Docampo, A. Goriely and H. J. Snaith, *Adv. Funct. Mater.*, 2014, **24**, 151-157.
7. A. Kojima, K. Teshima, Y. Shirai and T. Miyasaka, *J. Am. Chem. Soc.*, 2009, **131**, 6050-6051.
8. J.-H. Im, C.-R. Lee, J.-W. Lee, S.-W. Park and N.-G. Park, *Nanoscale*, 2011, **3**, 4088-4093.
9. J. Burschka, N. Pellet, S.-J. Moon, R. Humphry-Baker, P. Gao, M. K. Nazeeruddin and M. Gratzel, *Nature*, 2013, **499**, 316-319.
10. N. J. Jeon, J. H. Noh, Y. C. Kim, W. S. Yang, S. Ryu and S. I. Seok, *Nature materials*, 2014, **13**, 897-903.
11. M. Xiao, F. Huang, W. Huang, Y. Dkhissi, Y. Zhu, J. Etheridge, A. Gray-Weale, U. Bach, Y.-B. Cheng and L. Spiccia, *Angew. Chem.*, 2014, **126**, 10056-10061.
12. S. Mastroianni, F. D. Heinz, J. H. Im, W. Veurman, M. Padilla, M. C. Schubert, U. Wurfel, M. Gratzel, N. G. Park and A. Hinsch, *Nanoscale*, 2015, **7**, 19653-19662.
13. I. Horcas, R. Fernández, J. M. Gómez-Rodríguez, J. Colchero, J. Gómez-Herrero and A. M. Baro, *Rev. Sci. Instrum.*, 2007, **78**, 013705.
14. T. C. Sum, N. Mathews, G. Xing, S. S. Lim, W. K. Chong, D. Giovanni and H. A. Dewi, *Acc. Chem. Res.*, 2016, **49**, 294-302.
15. L. Wang, C. McCleese, A. Kovalsky, Y. Zhao and C. Burda, *J. Am. Chem. Soc.*, 2014, **136**, 12205-12208.
16. M. B. Price, J. Butkus, T. C. Jellicoe, A. Sadhanala, A. Briane, J. E. Halpert, K. Broch, J. M. Hodgkiss, R. H. Friend and F. Deschler, *Nature communications*, 2015, **6**, 8420.
17. Q. Chen, H. Zhou, Y. Fang, A. Z. Stieg, T.-B. Song, H.-H. Wang, X. Xu, Y. Liu, S. Lu, J. You and others, *Nature communications*, 2015, **6**, 7269.

18. G. Xing, N. Mathews, S. S. Lim, N. Yantara, X. Liu, D. Sabba, M. Grätzel, S. Mhaisalkar and T. C. Sum, *Nature Materials*, 2014, **13**, 476-480.
19. B.-E. Cohen, S. Aharon, A. Dymshits and L. Etgar, *The Journal of Physical Chemistry C*, 2016, **120**, 142-147.
20. X. Wu, M. T. Trinh, D. Niesner, H. Zhu, Z. Norman, J. S. Owen, O. Yaffe, B. J. Kudisch and X. Y. Zhu, *J. Am. Chem. Soc.*, 2015, **137**, 2089-2096.
21. D. Shi, V. Adinolfi, R. Comin, M. Yuan, E. Alarousu, A. Buin, Y. Chen, S. Hoogland, A. Rothenberger, K. Katsiev, Y. Losovyj, X. Zhang, P. A. Dowben, O. F. Mohammed, E. H. Sargent and O. M. Bakr, *Science*, 2015, **347**, 519-522.
22. Q. Dong, Y. Fang, Y. Shao, P. Mulligan, J. Qiu, L. Cao and J. Huang, *Science*, 2015, **347**, 967-970.
23. G. Xing, B. Wu, S. Chen, J. Chua, N. Yantara, S. Mhaisalkar, N. Mathews and T. C. Sum, *Small*, 2015, **11**, 3606-3613.
24. W.-J. Yin, T. Shi and Y. Yan, *Appl. Phys. Lett.*, 2014, **104**, 063903.